ISBN: 978-3-95450-206-6 doi:10.18429/JACoW-FLS2018-WEP2PT003

UNDULATOR PHASE MATCHING FOR THE THE EUROPEAN XFEL

Y. Li, J. Pflueger, European XFEL GmbH, Hamburg, Germany

Abstract

The undulator system in the European XFEL is mainly comprised 5-m long undulator segments and 1.1 m long intersections in between. In intersections the electron velocity is faster than it inside an undulator and the optical phase is detuned. The detune effect is also from the undulator fringe field where electron longitudinal speed also deviates from the oscillation condition. The total detune effect is compensated by a magnetic device called phase shifter, which is correspondingly set for a specific undulator gap. In this paper we introduce the method to set the phase shifter gap for each K parameter according to the measured magnetic field.

INTRODUCTION

High gain free electron lasers (FELs) using the principle of Self-Amplified Spontaneous Emission (SASE) are so far the only way to generate FEL radiation in the hard X-ray range [1-5]. For VUV radiation alternatives such as harmonic generation exist generate radiation which lead to increased stability [6]. However, aside from such differences both require long undulator systems with lengths from tens of meters up to about 200 meters depending on the radiation wavelength, electron beam and undulator parameters. Such a long undulator system cannot be built as a continuous device. For practical reasons of manufacturing it must be segmented into lengths around typically 5m maximum.

For the FEL process the interruption of the undulator implies a problem: The longitudinal speed of the electrons in the intersection is different to that inside the undulator and therefore the optical phase matching between laser field and electron motion is perturbed. In a fixed gap undulator system such as FLASH [1,2]or LCLS I [3] phase matching can be obtained by choosing the intersection length and tuning the end fields of the undulator segments properly. The phase matching in a gap tunable system is more complicated since the phase mismatch in the intersection changes with undulator gap. With a phase shifter, a small magnetic chicane, an additional delay is induced in the electron orbit. By properly selecting the phase shifter strength and hence the delay the optical phase can be matched at any gap [7].

The European X-ray free electron laser (EXFEL) facility [5] is a large project driven by a 1.8 kilometer long superconducting linac. The SASE FEL is used throughout the European XFEL. An electrons beam is accelerated up to maximum of 17.5 GeV. Then it is guided through the undulator system to generate high quality soft and hard X-rays. The radiation wavelength can be changed by variation of the undulator gap and in addition the beam energy: The hard X-ray range from 0.1 to 0.4 nm is covered by two undulator lines called SASE1 and SASE2. The soft X-Ray wavelength range from 0.4 to 1.6 nm is covered by one undulator line called SASE3.

For all SASE beam lines the undulators and phase shifters are well characterized before installation: Undulators were accurately tuned for small trajectory and phase errors in the operational gap range [8,9]. After tuning the characterization for each segment includes high resolution field maps as a function of gap in 0.5mm steps. They are the basis for the calculation of device properties such as K-Parameter, optical phase errors, trajectory wander etc. All phase shifters were well tuned and characterized as well [10-13].

An undulator system comprised of many segments is best controlled by the K-Parameter, which directly relates to the radiation wavelength, and not by the individual gaps, which differ slightly from segment to segment due to manufacturing and material tolerances. The K-parameter plays a key role and needs to be provided with an accuracy of $\Delta K/K \leq 2 \times 10^{-4}$.

PHASE MATCHING STRATEGY

Practical Situation

One feature of the undulator system for SASE FEL is that all segments must work cooperatively: In order not to deteriorate the FEL process the individual K-parameters need to be provided with an accuracy determined by $\Delta K/K \leq \rho$ where ρ is the Pierce parameter, which for EXFEL is about 2×10^{-4}. Therefore in an undulator system the gaps of individual undulator segments need to be adjusted so all match the same K.

On the other side field measurement on undulators is made by controlling the gap, which can be directly controlled mechanically with micrometer precision. Therefore, the K-parameters for each segment needs to be evaluated by interpolation from measurements made at different gaps.

Phase Matching Criteria

Figure 1 illustrates two undulator cells. Each cell is subdivided into four regions: On going from left to right the beginning of a cell is chosen in the field free region in the very left before the undulator. The region from at the beginning of the cell to the beginning of undulator bulk poles, including the drift space and the undulator fringe field, is called entrance fringe. The phase advance in this part is φ_{Entr}. The periodic field region inside the undulator is called bulk field. The phase advance over this region is φ_{Bulk}. Ideally at the first harmonic the phase advance in this region is 2π per period. Similar to the entrance fringe the region from the end of bulk field to the beginning of phase shifter is called exit fringe with the phase advance φ_{Exit}. In the field free region after the exit fringe the phase shifter is placed. The phase advance over the phase shifter is φ_{PS}. Since the phase shifter has very low fringe fields [7], it does not interfere with the undula-

ISBN: 978-3-95450-206-6 doi:10.18429/JACoW-FLS2018-WEP2PT003

tor and the spatial extension is very close to its physical length of 230mm only. The region after the phase shifter is again field free. Accordingly the phase advance over the first undulator cell can be written as $\varphi_{\text{Und},1} = \varphi_{\text{Entr},1} + \varphi_{\text{Bulk},1} + \varphi_{\text{Exit},1} + \varphi_{\text{PS},1}$.

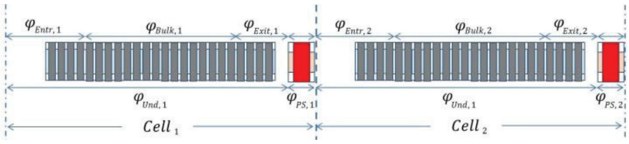

Figure 1: Definition of the different field regions in two sample undulator cells.

Only planar undulators are used at the European XFEL, so only the vertical field B_y plays a role. The horizontal field component B_x resulting from field errors is less than ≈ 10^{-3} times smaller than the main field component and can be neglected. The energy radiated per unit solid angle per unit frequency interval $dI(\omega)/d\Omega$ is $dI(\omega)/d\Omega = 2|A(\omega)|^2$ [14, 15]. The on-axis radiation of a planar undulator $A(\omega)$ is written as:

$$A(\omega) = i\left(\frac{e^2}{8\pi^2 c}\right)^{1/2} \frac{k}{\gamma} \int_0^z I_{1y}(z_1) e^{ik[\int_0^{z_1} \frac{1}{2\gamma^2}(1+I_{1y}^2(z_2)dz_2)]} dz_1, \quad (1)$$

where $k = \frac{2\pi}{\lambda_{Rad}}$ is the wave number, λ_{Rad} the radiation wavelength, c is the speed of light, e the electron charge and γ the kinetic energy in units of the electron rest mass. I_{1y} is the 1st field integral of B_y. The argument of the exponential function in Eq. (1) is the optical phase function [15]:

$$\varphi(z_1) = \int_0^{z_1} \frac{k}{2\gamma^2}(1 + I_{1y}^2(z_2)dz_2). \quad (2)$$

For convenience a normalized form of A, A_n, is used. In terms of the optical phase $\varphi(z_1)$ and the 1st field integral Eq. (1) is rewritten:

$$A_n = \int_0^z I_{1y}(z_1) e^{i\varphi(z_1)} dz_1. \quad (3)$$

A_n is complex. A_n for two undulator segments is the vector sum of two complex numbers. Using the normalized form is written as:

$$A_{n,sum} = A_{n,1} + e^{i(\varphi_{Und,1}+\varphi_{PS})} A_{n,2}, \quad (4)$$

where $A_{n,1}$ and $A_{n,2}$ denote A_n of the first and the second undulator, respectively. Both undulators and the corresponding radiation are similar but not identical. Each can be expressed in complex polar coordinates as:

$$A_n = |A_n| e^{i\psi}. \quad (5)$$

ψ is the phase of the radiation complex, A_n and must not be confused with the optical phase φ.

The total A_n of two undulators is the complex sum of two. Eq (4) is then rewritten as:

$$A_{n,sum} = |A_{n,1}| e^{i\psi_1} + |A_{n,2}| e^{i\psi_2} \cdot e^{i(\varphi_{Und,1}+\varphi_{PS})} \quad (6)$$

The maximum for $|A_{n,sum}|$ is obtained if the condition:

$$\psi_1 = \varphi_{und,1} + \varphi_{PS} + \psi_2 + 2n\pi \quad (7)$$

is fulfilled where n is an integer. Eq.(7) is the criterion for calculating the phase matching. Figure 2 gives an illustrative description. A_n of the two undulators are plotted in the complex plane. If Eq. (7) is fulfilled the resulting A_n is longest if $A_{n,1}$ and $A_{n,2}$ are collinear.

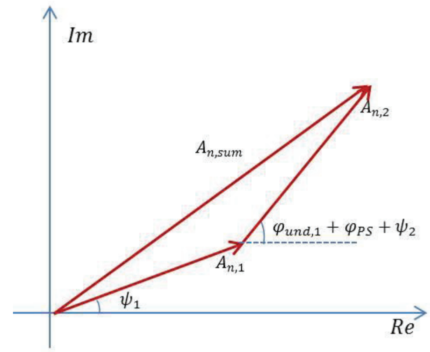

Figure 2: Sum of the A_n of two undulators. The length of A_n is maximum if the condition $\psi_1 = \varphi_{und,1} + \varphi_{PS} + \psi_2 + 2n\pi$ is satisfied.

In order to explain the relation between the phase of the complex A_n, ψ, and the optical phase φ, we analyse an undulator field comprised by an ideal bulk field and two ending field. Eq.(3) is expressed by the integral over different parts of an undulator as sketched in Figure 1:

$$A_n = \delta_{entr} + e^{i\varphi_{Entr}} \int_{L_{entr}}^{L_{entr}+L_{bulk}} I_{1y}(z_1) e^{i\varphi(z_1)} dz_1 + \delta_{exit}. \quad (8)$$

Where $\delta_{entr} = \int_0^{L_{entr}} I_{1y}(z_1) e^{i\varphi(z_1)} dz_1$, $\delta_{exit} = e^{i(\varphi_{Entr}+\varphi_{bulk})} \int_{L_{entr}+L_{bulk}}^{L_{entr}+L_{bulk}+L_{exit}} I_{1y}(z_1) e^{i\varphi(z_1)} dz_1$ are the contributions to A_n from the undulator end fields at the entrance and exit. In the end field sections the poles have different strength from the bulk and the optical field is out of resonance. δ_{entr} and δ_{exit} only contribute to the optical phase advance φ_{Entr} and φ_{Exit} but at resonance their contributions to the modulus of A_n are negligibly small. Therefore Eq. (8) is simplified:

$$A_n \approx e^{i\varphi_{Entr}} \int_{L_{entr}}^{L_{entr}+L_{bulk}} I_{1y}(z_1) e^{i\varphi(z_1)} dz_1. \quad (9)$$

The bulk field is expressed by sinus function and expressed in terms of Bessel functions [16]:

$$A_n \approx -e^{i\varphi_{Entr}} K \cdot N \frac{\lambda_u}{2} [J_0(\frac{K^2}{1+0.5K^2}) - J_1(\frac{K^2}{1+0.5K^2})]. \quad (10)$$

Where N is the number of periods. J_0 and J_1 are the Bessel functions of integer order 0 and 1.

Eq. (10) shows that the contribution from the bulk field to the vector potential is real, since the phase advance per period is 2π. Therefore $\varphi_{bulk} = 0$ and has no effect on the phase of A_s. So ψ, is determined by the entrance field of an undulator:

$$\psi = \varphi_{entr}. \quad (11)$$

Because in an ideal undulator $\varphi_{bulk} = 0$ and $\varphi_{und} = \varphi_{entr} + \varphi_{bulk} + \varphi_{exit}$, the criteria of Eq. (7) for phase matching can be written in the format of optical phase:

$$\varphi_{exit,1} + \varphi_{PS} + \varphi_{entr,2} = 2n\pi. \quad (12)$$

Eq. (12) gives a criterion for the phase matching of two undulators: The optical phase from the last bulk pole of the upstream undulator should change integral times of 2π to the first bulk pole of the next undulator. However, Eq. (12) assumes an ideal bulk field of the undulator with results in a phase advance of 2π per period over the whole undulator. In practice phase errors are unavoidable and the accuracy of Eq. (12) is affected by field errors.

ISBN: 978-3-95450-206-6 doi:10.18429/JACoW-FLS2018-WEP2PT003

MATCHING RESULTS

Comparison of K for Two Undulators

A SASE undulator system such as SASE1 or SASE2 of the European XFEL comprises 35 undulator segments and 34 phase shifters, which have to be matched together by applying the methods derived in the last section. For all these components accurate magnetic measurement data are available: For all undulators there are accurate high resolution field maps.

For demonstration of the method two undulator segments, the U40-X005 and the U40-X006 and one phase shifter, the PS073, are used. The K-parameter of the two undulators is set from 1.5 up to 3.9 with a step size of 0.2. The gap for each segment was fitted to match the desired K-parameter. Fig. 3 illustrates the required gap of the two segments as a function of K. The blue curve shows the difference. It is seen that there is an almost constant difference of about 0.15 mm with a very slight variation with gap. It is due to differences in the mechanics, encoder initialization and magnet structure and shows the need of individual gap adjustment. This is a quite representative for other undulator segments as well.

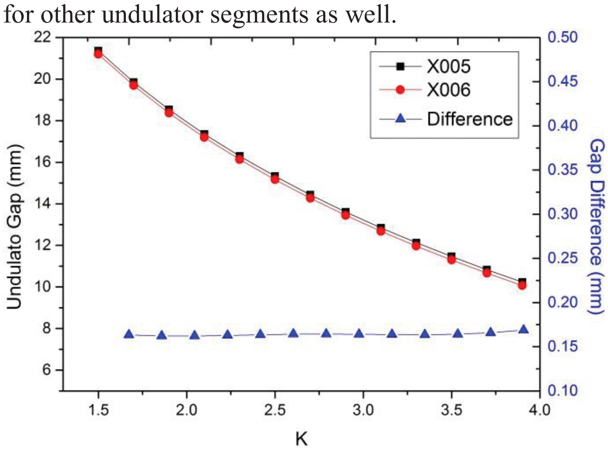

Figure 3: Gap vs. K-parameter for the U40-X005, black squares, and U40-X006, red circles. The difference is shown by the blue triangles.

Phase Matching using the A_n

The condition for proper phase matching is defined by Eq. (7). The real and imaginary part of the normalized A_n using Eq (3) and the phase ψ, can be calculated. Figure 4 demonstrates the phase matching using the hodograph representation.

The abscissa represents the real and the y-axis the imaginary part in arbitrary units. Two cases representing the maximum and minimum K values, 3.9 and 1.7, are chosen for demonstration. Going along a perfect undulator the complex evolves along a straight line starting at 0. For each K value, two conditions called 'matched' and 'anti-matched' are shown. 'Matched' fulfils the phase matching condition, Eq. (7) i.e. 2nπ. For the 'Anti-matched' condition the phase delay between the undulators is (2n+1) π. Results are shown by the left and right plots, respectively. The start angle is different to various K value and it depends on the entrance ending field. It is seen that in the matched condition the A_n of two the undulators, U40-X005 and U40-X006, have the same in length and point in exactly the same direction and the total length of the radiation from two undulators is twice the length of a single one and reaches the maximum intensity as illustrated in Figure 2. In contrast as seen by the right plot in the anti-matched condition A_n of the two undulators have again the same length but reverse direction. Therefore the total length is zero. It should be emphasized that this applies to the forward direction only. The effect of residual field errors is seen by some small wiggles on the lines and resulting small deviations from perfect straightness.

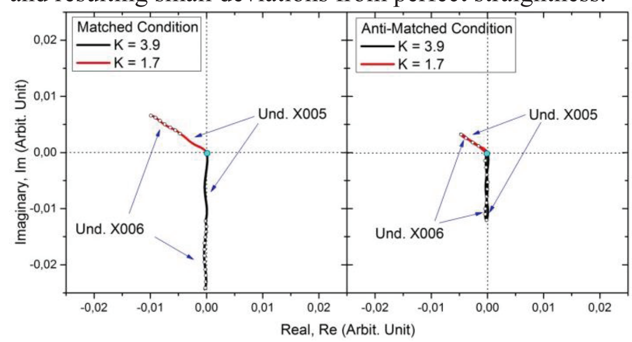

Figure 4: Hodograph of the real and imaginary part of the radiation A_n for two K values. The left plot corresponds matched phasing with 2nπ phase difference. The right plot corresponds anti-matched phasing with (2n+1)π phase difference leading to zero amplitude in forward direction.

Small differences in the ending fields as well as small individual differences in the phase shifter require strict matching of undulators and phase shifters. Figure 5 shows the required phase shifter gap as a function of the undulator K-parameter. The phase shifter can be operated on different phase numbers, ν, [7]. In order to have a sufficiently large tuning range over the whole operational K harmonic number $\nu = 14$ or larger needs to be used. Fig. 5 shows the results. Each curve corresponds to a specific harmonic number. It is seen that the larger the harmonic number the larger the K range. However at large K the space between the curves gets smaller and the phase gets more sensitive to the phase shifter gap.

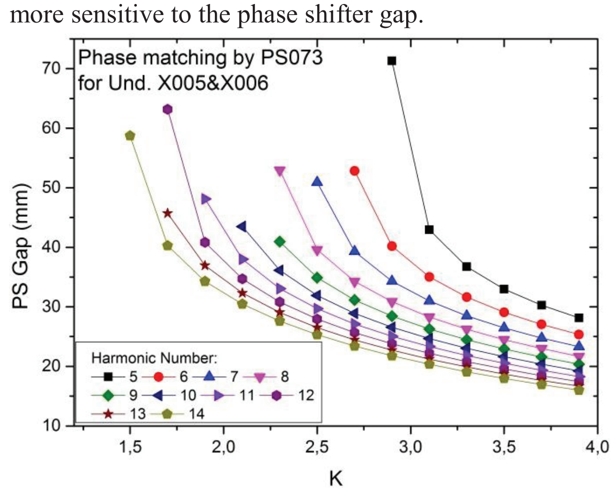

Figure 5: The required gap of phase shifter PS073 placed between U40-X005 and U40-X006 as a function of the K-

ISBN: 978-3-95450-206-6 doi:10.18429/JACoW-FLS2018-WEP2PT003

parameter. The individual curves correspond to different phase numbers. Continuous tuning over the whole K-range requires harmonic numbers ≥14.

Phase Matching by Pole

Phase matching described so far is the most general treatment which based on the complex A_n of the two undulators calculated from their measured fields. Under the assumption that the bulk structure has zero phase error there is a simple alternative using Eq. (12). Only the end field contributes. In reality the problem arises how to select the boundary between bulk and end fields. The applicability of this simplification was again tested using the undulators U40-X005 and U40-X006 and the phase shifter PS073.

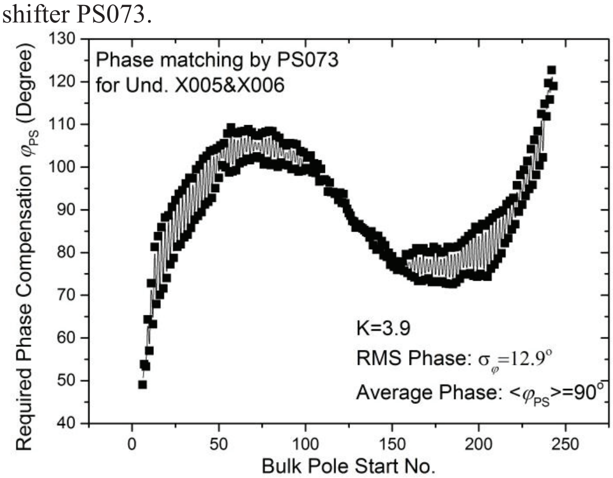

Figure 6: Phase compensation as function of the pole number where the bulk field starts.

Figure 6 shows the required phase compensation of the phase shifter as function of the pole number where the bulk structure starts. It is seen that depending on the start the phase varies significantly from about 50 to 120 degrees with an RMS value of 12.9 degrees. There is no hard criterion to select a specific pole as the start pole for the bulk field. In the bulk structure there is a systematic deviation from a 2π phase advance per period. The explanation is that on all European XFEL undulators small parabolic girder deformations have been observed, which result from changing magnetic forces but they are well within the specifications. Therefore different extensions of the bulk field leads to different phase matching requirements [10]. Since the curve in Figure 6 has some symmetry averaging can be used. The average of the requested phase in Figure 6 is 90° and is used to calculate the phase shifter gap. Now, using Eq. (12) phase shifter gap settings in full analogy to Fig. 5 can be calculated.

Both methods provide comparable results. Instead of reproducing curves such as in Figure 5 a quantitative analysis is given in Figure 7. The black curve shows the difference of the phase shifter gap setting a function of the undulator K-parameter. It does not exceed -7µm. As shown by the blue curve the difference of the phase shifter correction is less than one degree. These differences are negligible and both methods give the same phase matching and can be used for the work.

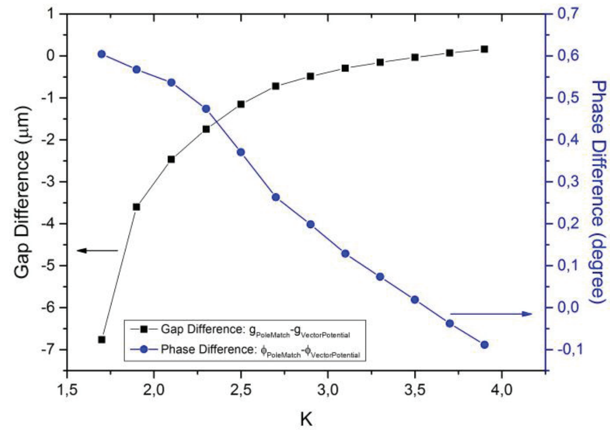

Figure 7: Comparison between the results of two matching criteria. The black curve shows the difference of the required phase shifter gap, the blue curve the phase difference of phase shifter.

CONCLUSION

In this paper the theoretical basis for the proper matching the optical phase of different tuneable undulator segments with the help of phase shifters are worked out. It is used in large distributed undulator systems for SASE FELs. Two matching methods, based on the undulator on-axis radiation and the optical phase, are derived and compared. We prove to the undulator with identical bulk field these two methods are equivalent.

The matching results for two undulator segements in SASE1 are shown as the example. The Gap-K curves for 2nπ phase matching are illustrated and compared.

REFERENCES

[1] “A VUV Free Electron Laser at the TESLA Test Facility” Conceptual Design Report, TESLA-FEL 95-03 (1995)

[2] B. Faatz *et. al.* Nucl. Instr. and Meth. A635(2011) 52

[3] Linac Coherent Light Source, (LCLS I), Conceptual Design Report SLAC-R-593 UC-414, 2002 available under: http://www.slac.stanford.edu/cgi-wrap/getdoc/slac-r-593.pdf

[4] Linac Coherent Light Source II (LCLS-II) Conceptual Design Report, SLAC-R-978; I-060-003-000-00, 2011 available under: http://www.slac.stanford.edu/pubs/slacreports/reports19/slac-r-978.pdf

[5] M. Altarelli *et al.*, “The European X-ray Free-electron Laser”, Technical Design Report, ISBN 3-935702-17-5, 2006; http://www.xfel.eu/dokumente/technical_documents

[6] The FERMI Project at Elletra, Conceptual Design Report, **ST/F-TN-07/12 (2007).** Available under: https://www.elettra.trieste.it/lightsources/fermi/fermi-machine/fermicdr.html

ISBN: 978-3-95450-206-6 doi:10.18429/JACoW-FLS2018-WEP2PT003

[7] H. Lu, Y. Li, J. Pflueger, "The permanent magnet phase shifter for the European X-ray Free Electron Laser", *Nucl. Instr. and Meth. A* 605 (2009) 399

[8] J. Pflueger, et. al. Proceedings of the FEL2013, August 25-30, New York City, USA, Paper TUPSO60

[9] Y. Li, S. Abeghyan, K. Berndgen, M. Bagha-Shanjani, G. Deron, U. Englisch, S. Karabekyab, B. Ketenoglu, M. Knoll, F. Wolff-Fabris, M. Viehweger, M. Yakopov, J. Pflueger, "Magnetic Measurement Techniques for the Large-Scale Production of Undulator Segments for the European XFEL" Synchrotron Radiation News, Vol. 28, Nr. 3, 2015

[10] Y. Li, B. Ketenoglu, J. Pflueger, "Girder deformation related phase errors on the undulators for the European X-Ray Free Electron Laser", *Phys. Rev. ST-AB* 18, 060704 (2015)

[11] Y. Yang, Y. Li, H. Lu, F. Wolff-Fabris, J. Pflueger, "Shimming Strategy for the Phase Shifters used in the European XFEL", Contribution TUPSO42, FEL2013, Aug 25-30, 2013, New York, USA

[12] Y. Li, J. Pflueger, "High Accuracy shimming technique for the Phase Shifters of the European XFEL", MOPS007, *FEL2014,* August 25-29, Basel , Switzerland

[13] Y. Li, J. Pflueger, "Tuning method for phase shifters with very low first field integral errors for the European X-ray Free Electron Laser" , *Phys. Rev. ST-AB* 8, 030703 (2015)

[14] J. D. Jackson, "Classical Electrodynamics", Chapter 14, John Wiley & Sons Inc, New York, 1962

[15] R.P. Walker, "Interference effects in undulator and wiggler radiation sources", *Nucl. Instr. and Meth.* A335 (1993) 328

[16] S. Krinsky, M.L. Perlman, R.E. Watson in: Handbook of Synchrotron Radiation, Vol 1 Eds. E.E Koch, D.E. Eastmans, Y. Farge *et al*. Chapter 2, North Holland Publishing Company, Amsterdam, 1983